

Observation of discrete vortex solitons in optically-induced photonic lattices

Dragomir N. Neshev, Tristram J. Alexander, Elena A. Ostrovskaya, and Yuri S. Kivshar
 Nonlinear Physics Group, Research School of Physical Sciences and Engineering,
 Australian National University, Canberra ACT 0200, Australia

Hector Martin and Zhigang Chen
 Department of Physics and Astronomy, San Francisco State University,
 CA 94132 and TEDA College, Nankai University, China

We study, both theoretically and experimentally, the interaction of an optical beam carrying a phase dislocation (an optical vortex) with a two-dimensional optically-induced lattice. We demonstrate strong stabilization of optical vortices by the lattice discreteness in a self-focusing nonlinear medium, and generate spatially localized structures in the form of discrete vortex solitons.

PACS numbers: 42.65.Tg, 42.65.Jx, 42.70.Qs

Periodic photonic structures and photonic crystals recently attracted a lot of interest due to the unique ways they offer for controlling light propagation. Periodic modulation of the refractive index modifies the wave diffraction properties and strongly affects nonlinear propagation and localization of light [1]. Recently, many nonlinear effects, including formation of lattice solitons, have been demonstrated experimentally for one- and two-dimensional optically-induced photonic lattices [2, 3, 4, 5]. The concept of optically-induced lattices [6] arises from the possibility to modify the refractive index of a nonlinear medium with periodic optical patterns, and use a weaker probe beam to study scattering of light from the resulting periodic photonic structure. Current experiments employ photorefractive crystals with strong electro-optic anisotropy to create a linear optically-induced lattice with a polarization orthogonal to that of a probe beam, which also eliminates the nonlinear interaction between the beam and the lattice.

So far, only simple stationary structures have been described theoretically and generated experimentally in optically-induced lattices [2, 3, 4, 5, 6]. One of the most important next steps is the study of nonlinear modes with a nontrivial phase such as vortices, the fundamental localized objects appearing in many branches of physics. In optics, vortices are associated with the phase singularities carried by diffracting optical beams [7]. When such vortices propagate in defocusing nonlinear Kerr-like media, the vortex core with a phase singularity becomes self-trapped, and the resulting structure is known as an optical vortex soliton [1]. Such vortex solitons are usually generated experimentally within broad diffracting beams, e.g. by using a phase mask [8, 9], and they demonstrate many similarities with the vortices observed in superfluids and Bose-Einstein condensates.

In contrast, optical vortices do not exist in a self-focusing nonlinear medium: a ring-like optical beam with a phase dislocation carrying a finite orbital angular momentum [10] decays into the fundamental solitons lying on the main ring [11]. This effect was first observed experimentally in the saturable Kerr-like nonlinear me-

dia [12], and then in photorefractive [9] and quadratic [13] nonlinear media in the self-focusing regime.

Recent theoretical studies of the discrete [14] and continuous models with an external periodic potential [15] suggest that the vortex-like structures can be stabilized by the lattice discreteness. In this Letter, we report the first experimental observation of discrete vortex solitons and demonstrate, both theoretically and experimentally, that optical vortices can be stabilized in a self-focusing nonlinear media by a two-dimensional periodic potential of a photonic lattice.

To lay a background for our experiment, we study numerically the propagation of a vortex beam in a two-dimensional optically induced photonic lattice induced in a nonlinear photorefractive material. Following Refs. [4, 6], we model a photorefractive crystal externally biased with a DC field along its extraordinary x-axis (crystalline c-axis). An optically-induced two-dimensional refractive index grating is created in the crystal via the photorefractive effect, by a periodic partially coherent pattern created with a wide input beam of high intensity, polarized along the ordinary y-axis [16]. Since the electro-optic coefficients of the SBN crystal for ordinary polarization are small, the grating can be treated as linear and constant along the propagation axis z. The effectively two-dimensional square grating, created by the ordinary beam with wavelength λ can be modelled by the intensity pattern $I_g = I_0 \sin^2(x/\lambda) \sin^2(y/\lambda)$, where $\lambda = 2\pi/K = n_0 k_0 \sin \theta$, θ is the angle between the input wave and the z-axis, $k_0 = 2\pi/\lambda$, and n_0 is the refractive index along the ordinary axis.

The probe beam propagating through this two-dimensional photonic structure is extraordinary polarized [6], which for the strongly electro-optically anisotropic crystal ensures both its nonlinear propagation and negligible back-action on the grating. Then, within the approximation of isotropic nonlinearity, the evolution of a probe beam is governed by the following nonlinear equation

$$2ik_1 \frac{\partial E}{\partial z} + \Delta_{\perp} E - k_0^2 n_e^4 r_{33} E_{sc} E = 0; \quad (1)$$

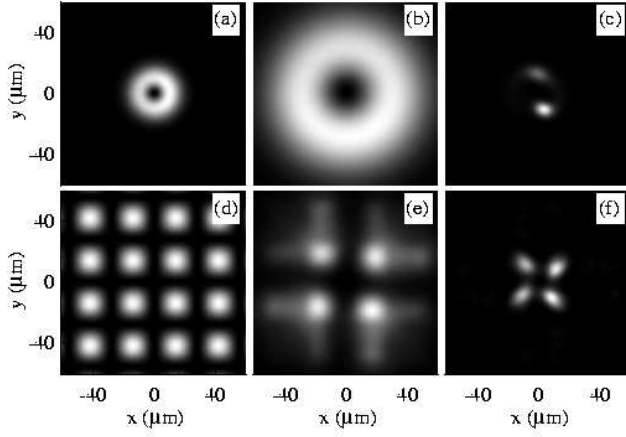


FIG. 1: Numerical results. (a,d) Input vortex (top) with the peak intensity one fifth that of the linear lattice (bottom), $I_0 = 3I_d$. Top (b,c) and bottom (e,f) panels show the results of vortex propagation without and with the lattice, respectively. (b,e) Linear diffraction, with the nonlinearity of the probe beam neglected with $V_0 = 2.7$. (c,f) Nonlinear propagation with $V_0 = 24.13$.

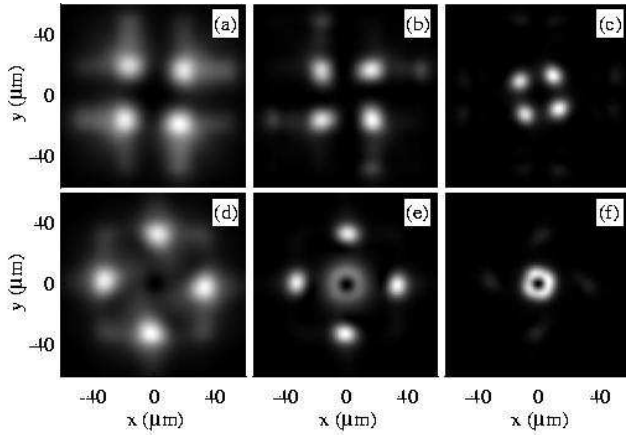


FIG. 2: Numerical results. Dependence of the evolution of the input vortex [see Fig. 1 (a)] on the strength of the nonlinearity, V_0 (or applied bias field). (a-c) Vortex center is at the maximum of the effective periodic potential; (d-f) vortex center is at the minimum of the effective potential. The value of V_0 is: (a,d) $V_0 = 2.7$, (b,e) $V_0 = 8.04$ and (c,f) $V_0 = 16.09$.

where ∇^2 is the two-dimensional Laplacian, n_e is the refractive index along the extraordinary axis, $k_1 = k_0 n_e$, and E_{sc} is the space-charge field, $E_{sc} = E_0(1 + I)$, expressed through the total intensity, $I = |\mathbf{E}|^2 + I_g$, normalized with respect to the dark irradiance of the crystal, I_d . For our choice of the polarity of the biasing DC field E_0 , the nonlinearity exhibited by the probe beam is self-focusing, i.e. $n_1 - k_0^2 n_e^4 r_{33} E_0 > 0$.

By measuring the transverse coordinates in the units of the half-period of the induced grating x_0 , and the propagation distance in the units of $k_1 x_0^2$, Eq. (1) can be written

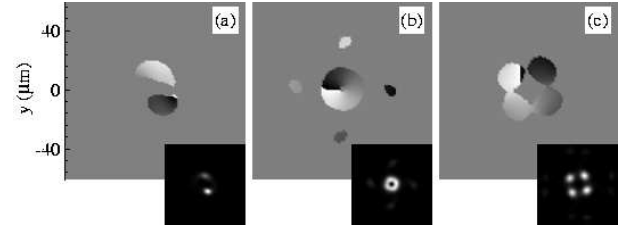


FIG. 3: (a,b) The beam phase after the vortex decay or collapse, as presented in Fig. 1 (c) and Fig. 2 (f), respectively, and (c) the phase of the discrete vortex soliton shown in Fig. 2 (c). Black corresponds to a phase of $\phi = 0$, white to $\phi = 2\pi$. For clarity, phase information is only shown for beam intensities greater than $0.2I_d$ in (a) and $0.1I_d$ in (b,c). Insets show the corresponding beam intensities.

in the dimensionless form :

$$i \frac{\partial u}{\partial z} + \frac{1}{2} \nabla^2 u - \frac{V_0 u}{1 + I(x;y) + |u|^2} = 0; \quad (2)$$

where $V_0 = n_1 x_0^2 = 2$, with $V_0 = 1$ corresponding to a bias field of 74.6 V/cm , and the normalized grating intensity is $I(x;y) = I_0 \sin^2(x/2) \sin^2(y/2)$. In our numerical simulations we assume the normalization consistent with the parameters of our experiment. Consequently, $x = 1$ corresponds to $14 \text{ }\mu\text{m}$ and the typical value $z = 1.4$ corresponds to the propagation distance of 8.2 mm .

As an initial condition, we use a radially-symmetric input beam carrying a phase dislocation, $u(r; \theta) = a \exp(-w r^2 + i \theta)$, with $a = 1.8$ and $w = 1$, which corresponds to a peak intensity roughly one fifth of the typical lattice potential. The angular phase, θ , is varied from 0 to 2π to generate a vortex with unit topological charge. In all simulations, the vortex is perturbed asymmetrically by a weak perturbation less than 5% of the maximum intensity, to facilitate development of azimuthal instabilities.

First, we study the propagation of the vortex beam without the lattice potential. In the absence of nonlinearity, the input beam diffracts, as shown in Fig. 1 (b). In the presence of a bias field, i.e. in a nonlinear self-focusing medium, the vortex decays into a diverging pair of solitons [see Fig. 1 (c)]. This type of decay (fragmentation), induced by azimuthal instability, is generic for a vortex-carrying beam, however the exact number of fragments depends on the parameters of the input beam. The fragments tend to rotate and move away from each other due to the phase and angular momentum carried by the vortex beam [9, 12, 13].

In the presence of a two-dimensional lattice potential and weak nonlinearity, the vortex exhibits the effect of discrete diffraction, whereby the power of the optical beam tends to distribute between many neighbouring lattice sites, as shown in Fig. 1 (e). Remarkably, for a stronger nonlinearity, the input beam does not decay or diffract, but transforms into a four-lobe structure trapped by the lattice [see Fig. 1 (f)] corresponding to the discrete vortex soliton [14, 15].

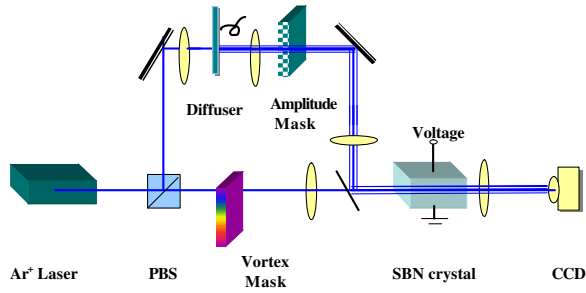


FIG. 4: Experimental setup for the observation of the discrete vortex solitons. PBS: Polarizing beam splitter, SBN: Strontium Barium Niobate crystal.

To study the effect of the lattice potential in more detail, we shift the center of the input vortex relative to the lattice, and vary the strength of the effective nonlinearity, V_0 , which in physical terms means varying the external bias field. Figures 2 (a-f) show the result of the vortex propagation in the lattice with two different input positions, for different strengths of the nonlinearity. When the vortex center is at the maximum of the effective potential (i.e. at the intensity minimum of the grating), discrete diffraction occurs [2 (a)] at a relatively low bias. A discrete vortex is generated for stronger bias fields [2 (b,c)], and its confinement by the lattice varies with the nonlinearity. Here, the four lobes of the discrete vortex are trapped by the neighboring minima of the potential, and the structure is stabilized by the lattice. However, when the vortex center is placed initially at the minimum of the effective potential (i.e. at the intensity maximum of the grating), the vortex either decays [2 (d,e)] or collapses [2 (f)].

In order to verify that the structure created by the input singular beam in the lattice resembles closely the discrete vortex soliton, in Figs. 3 (a-c) we compare the beam phase for the three cases of the vortex evolution. In full agreement with earlier studies [14, 15], the generated discrete vortex soliton is composed of four lobes with a total phase ramp of 2π , as shown in Fig. 3 (c).

Our experimental setup (Fig. 4), is similar to that reported in Refs. [5, 16]. An argon ion laser beam (operating at the wavelength $\lambda = 488 \text{ nm}$) is collimated and then split with a polarizing beam splitter. The ordinarily-polarized beam (o-beam) is focused onto a rotating diffuser, turning into a partially spatially incoherent source. A biased photorefractive crystal (SBN:60, $5.5 \times 5.8 \text{ mm}^3$, with $r_{33} = 280 \text{ pm/V}$) is employed to provide a self-focusing noninstantaneous nonlinearity, as in the previous demonstrations of the incoherent spatial solitons [17].

To generate a two-dimensional photonic lattice, we use an amplitude mask to modulate spatially the otherwise uniform o-beam after the diffuser. The mask is then imaged onto the input face of the crystal, thus creating a partially coherent pixel-like input intensity pattern [16]. The extraordinarily-polarized probe beam (e-beam) is

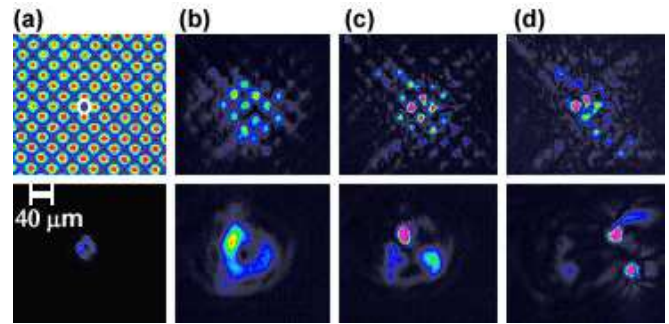


FIG. 5: Experimental observation of an optical vortex propagating with (top) and without (bottom) an optically-induced lattice. Shown in (a) are the intensity patterns of the lattice beam (top) and the vortex beam (bottom) at crystal input. Shown in (b-d) are the intensity patterns of the vortex beam at crystal output with a bias field of 600, 1200, and 3000 V/cm, respectively. The bright ring in the lattice pattern (a) indicates the location of the vortex at the input.

sent through a transmission vortex mask with unit topological charge, and then focused onto the crystal input face, propagating collinearly with the lattice. In addition, a uniform incoherent background beam (not shown in the figure) is used as "dark illumination" for re-tuning the nonlinearity. The input and output faces of the crystal are monitored with an imaging lens and a CCD camera.

Typical experimental results are summarized in Figs. 5 (a-d). A two-dimensional square lattice was first created, with its principal axes oriented in the diagonal directions shown in the top panel of Fig. 5 (a). Since the lattice has a spatial period of only $28 \mu\text{m}$, this orientation favors stable lattice formation. (A square lattice with its principal axes oriented in the x - y directions tends to suffer distortion due to anisotropic photorefractive nonlinearity.) In addition, the lattice beam is partially spatially incoherent, (spatial coherence length $\sim 100 \mu\text{m}$), which also entails stable lattice formation due to suppression of incoherent modulation instability [18]. The resulting periodic structure acts as a square array of optically induced waveguides for a probe beam. The vortex beam, shown in the bottom panel of Fig. 5 (a), was then launched straight into the middle of the lattice "cell" of four waveguides, as indicated by a bright ring in the lattice pattern. The vortex beam is coherent, e-polarized, and has the intensity about 5 times weaker than that of the lattice. In this geometrical configuration, the o-polarized lattice exhibits only a weak nonlinearity as compared to that experienced by the e-polarized vortex beam, and therefore remains nearly invariant as the bias field increases, with only a slight increase of its intensity contrast. Due to weak coupling between closely spaced waveguides of the lattice, the vortex beam exhibits discrete diffraction when the nonlinearity is low, whereas it forms a discrete vortex soliton at an appropriate level of higher nonlinearity. In the top panel of Fig. 5 (b), discrete diffraction of the vortex beam in the lattice was observed at a low bias field

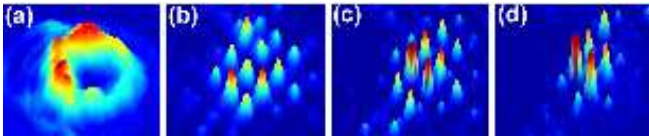


FIG. 6: Three-dimensional intensity patterns of the vortex beam showing: (a) vortex normal diffraction without the lattice, (b) discrete diffraction, (c) discrete focusing, and (d) the formation of a discrete vortex soliton in a two-dimensional optically-induced lattice.

of 600 V/cm . When the bias field was increased to 1200 V/cm [see Fig. 5 (c), the top panel], partial focusing of the vortex beam was observed (in the numerical simulations formation of a discrete vortex occurs already at this bias level). In this case, more energy of the vortex beam goes to the central four sites, but the side lobes still share a significant amount of the energy. Importantly, for higher nonlinearity, i.e. at a bias field of 3000 V/cm , a discrete vortex soliton is clearly observed [see Fig. 5 (d), top], with most of the energy concentrated at the central four sites along the principal axes of the lattice, indicating that a delicate balance has been reached between the discrete diffraction and self-focusing experienced by the vortex.

As predicted, the observed discrete diffraction and discrete self-trapping of the vortex beam in the photonic lattice is remarkably different from that in a homogeneous medium. In Fig. 5 (bottom row), we show the output intensity pattern of the vortex beam without the lattice, but under the influence of the same bias field (i.e. nonlinearity). At low bias of 600 V/cm , the vortex beam is slightly modulated, but maintains a doughnut-like diffraction pattern [Fig. 5 (b)]. At a higher bias of 1200 V/cm , the vortex beam breaks up into several

elements due to azimuthal instability in the self-focusing crystal [Fig. 5 (c)]. Another significant difference is that, as shown in the bottom panel of Fig. 5 (d), the two major soliton elements move away after breakup from their original locations towards the direction of crystalline c -axis due to the diffusion-induced self-bending enhanced by the high bias field [9]. In contrast, the vortex beam is well trapped by the periodic potential of the lattice (as shown in the top panels of Fig. 5), which suppresses the rich instability-induced dynamics (rotating, diverging and self-bending) of the elements in a continuous nonlinear medium. This behaviour can also be observed in the steady-state intensity patterns illustrated in Fig. 6, where the first picture shows the linear diffraction of the vortex in the continuous medium, and the other three show the discrete diffraction, discrete self-focusing, and self-trapping in the photonic lattice corresponding to the two-dimensional transverse patterns [see Figs. 5 (b-d), top].

In conclusion, we have numerically studied propagation of an optical beam with phase dislocation in a periodic two-dimensional photonic structure, and predicted the stabilizing effect of the lattice discreteness on the vortex propagation. We have observed experimentally the formation of a stable discrete optical vortex in two-dimensional optically-induced photonic lattices. The vortex has been created in a self-focusing nonlinear medium, and it was confirmed that the lattice provides a strong stabilization mechanism for the vortex which is transformed into a non-diffracting four-lobe stationary discrete structure with an alternating phase pattern.

This work was supported by the Australian Research Council, U.S. AFO SR (F49620-03-1-0299), and the Outstanding Overseas Chinese Young Investigator Award.

-
- [1] Yu.S. Kivshar and G.P. Agrawal, *Optical Solitons: From Fibers to Photonic Crystals* (Academic, San Diego, 2003).
- [2] J.W. Fleischer, T. Carmon, M. Segev, N.K. Efremidis, and D.N. Christodoulides, *Phys. Rev. Lett.* 90, 023902 (2003).
- [3] D. Neshev, E.A. Ostrovskaya, Yu.S. Kivshar, and W. Krokolkowski, *Opt. Lett.* 28, 710 (2003).
- [4] J.W. Fleischer, M. Segev, N.K. Efremidis, and D.N. Christodoulides, *Nature* 422, 147 (2003).
- [5] H. Martin, E.D. Eugenieva, Z. Chen, and D.N. Christodoulides, *arXiv: nlin.PS/0307047* (2003).
- [6] N.K. Efremidis, S. Sears, D.N. Christodoulides, J.W. Fleischer, and M. Segev, *Phys. Rev. E* 66, 046602 (2002).
- [7] See M.S. Soskin and M.V. Vlasov, in *Progress in Optics*, Vol. 42, Ed. E. Wolf (Elsevier, Amsterdam, 2001).
- [8] G.A. Swartzlander and C.T. Law, *Phys. Rev. Lett.* 69, 2503 (1992).
- [9] Z. Chen, M. Shih, M. Segev, D.W. Wilson, R.E. Muller, and P.D. Maker, *Opt. Lett.* 22, 1751 (1997).
- [10] V.I. Kruglov and R.A. Vlasov, *Phys. Lett. A* 111, 401 (1985).
- [11] W.J. Firth and D.V. Skryabin, *Phys. Rev. Lett.* 79, 2450 (1997); D.V. Skryabin and W.J. Firth, *Phys. Rev. E* 58, 3916 (1998).
- [12] V. Tikhonenko, J. Christou, and B. Luther-Davies, *J. Opt. Soc. Am. B* 12, 2046 (1995); *Phys. Rev. Lett.* 76, 2698 (1996).
- [13] D.V. Petrov, L. Torner, J. Martorell, R. Vilaseca, J.P. Torres, and C. Cojocaru, *Opt. Lett.* 23, 1444 (1998).
- [14] B.A. Malomed and P.G. Kevrekidis, *Phys. Rev. E* 64, 026601 (2001); P.G. Kevrekidis, B.A. Malomed, A.R. Bishop, and D.J. Frantzeskakis, *Phys. Rev. E* 65, 016605 (2001); P.G. Kevrekidis, B.A. Malomed, and Yu.B. Gaididei, *Phys. Rev. E* 66, 016609 (2002).
- [15] J. Yang and Z. Musslimani, *arXiv: physics/0304047* (2003), to be published in *Optics Letters*.
- [16] Z. Chen and K.M. McCarthy, *Opt. Lett.* 27, 2019 (2002).
- [17] M. Mitchell, Z. Chen, M. Shih, and M. Segev, *Phys. Rev. Lett.* 77, 490 (1996); Z. Chen, M. Mitchell, M. Segev, T.H. Coskun, and D.N. Christodoulides, *Science* 280, 889 (1998).
- [18] M. Soljacić, M. Segev, T. Coskun, D.N. Christodoulides,

and A . V ishwanath, Phys. Rev. Lett. 84, 467 (2000).
[19] See, e.g., S.R. Singh and D N . Christodoulides, Opt.

Comm . 118, 569 (1995).